Hindawi
International Journal of Antennas and Propagation
Volume 2021, Article ID 7334206, 8 pages
https://doi.org/10.1155/2021/7334206

Research Article

Small Antenna Design of Triple Band for WIFI 6E and WLAN Applications in the Narrow Border Laptop Computer

Wei-Chiang Jhang and Jwo-Shiun Sun

Department of Electronic Engineering, National Taipei University of Technology, Taipei, Taiwan

Correspondence should be addressed to Wei-Chiang Jhang; t106369006@ntut.edu.tw

Received 9 April 2021; Revised 29 June 2021; Accepted 1 July 2021; Published 9 July 2021

Academic Editor: Giacomo Oliveri

This paper presents the design of a small antenna for use in a wireless local area network (WLAN) and Wi-fi 6E on a narrow-border laptop. The dimensions of the antenna are $43 \times 3 \times 0.4\,mm^3$, and it features a grounding system simulated by a $200 \times 260\,mm^2$ copper plate. At low-frequency bands, a couple-fed right arm can excite the fundamental at 2.45 GHz in the $\lambda/4$ resonant mode to cover the range of 2.4–2.848 GHz. At higher bands, the couple-fed left arm and direct-fed right arm can control the higher $3\lambda/4$ mode at 5.825 GHz and $5\lambda/4$ mode at 6.85 GHz. The direct-fed left arm excites the fundamental at 5.16 GHz in the $\lambda/4$ resonant mode and, with integration of 5.16, 5.825, and 6.85 GHz, can fully cover the range of 5.15–7.125 GHz. In far-field measurements, the peak gain and efficiency in a WLAN with Wi-Fi 6E were 0.82 and 2.58 dBi and 53% and 68% in the low and high bands, respectively. Overall, the experiments revealed that the antenna exhibits a sufficient level of performance for a narrow-border laptop.

1. Introduction

High-speed data rates are the most effective solution with wireless local area network (WLAN) called authorize user wireless mobility. However, with the current technology of wireless systems, high-speed downloads are limited in applications such as the Internet of things and 4K and 8K video. The end users of such products consider the upload and download speeds of WLANs to be unsatisfactory. Therefore, the Wi-fi 6E (the sixth generation of Wi-fi) standard will be introduced in 2021. The bandwidth of Wi-fi 6E is between 5.925 and 7.125 GHz, with 14×80 or 7×160 MHz channels. Wi-fi functionality is essential for most wireless laptop features. Therefore, laptops should be outfitted with Wi-fi 6E. In the current market, the screen-to-body ratio provides useful information to the consumer. However, the spacing of the border area is limited because less than 4 mm is reserved for antennas. Studies [1–4] have discovered that the guidelines for designing WLAN antennas with coplanar waveguide, slot, and bend-type architectures cannot be implemented because of limited dimensions. In [5], small dimensions and a meandering shape with loop-type antennas were used. Other studies have investigated designs such as PIFA or monopole antennas for Wi-fi applications [6–9]. In [10–12], the authors used chip element to achieve small size and narrow boarder antenna design. However, the used of the inductor makes the hardware complex and also increases the difficulty of the manufacturing process. This study designed an antenna to perform in low-frequency (2.4–2.484 GHz) to high-frequency (5.925–7.125 GHz) bands by using a direct-fed arm and a couple-fed arm to enable full functionality in WLAN and Wi-fi 6E applications.

2. Antenna Design

Figures 1(a)–1(c) presents the antenna's FR4 basic construction. Tables 1 and 2 present the dimensions for optimal performance. Figure 2 presents photos from the construction and fabrication of the prototype antenna, in which the substrate's dielectric constant, loss tangent, and thickness are 4.4, 0.02, and 0.4 mm, respectively. A 33.02-cm-screen

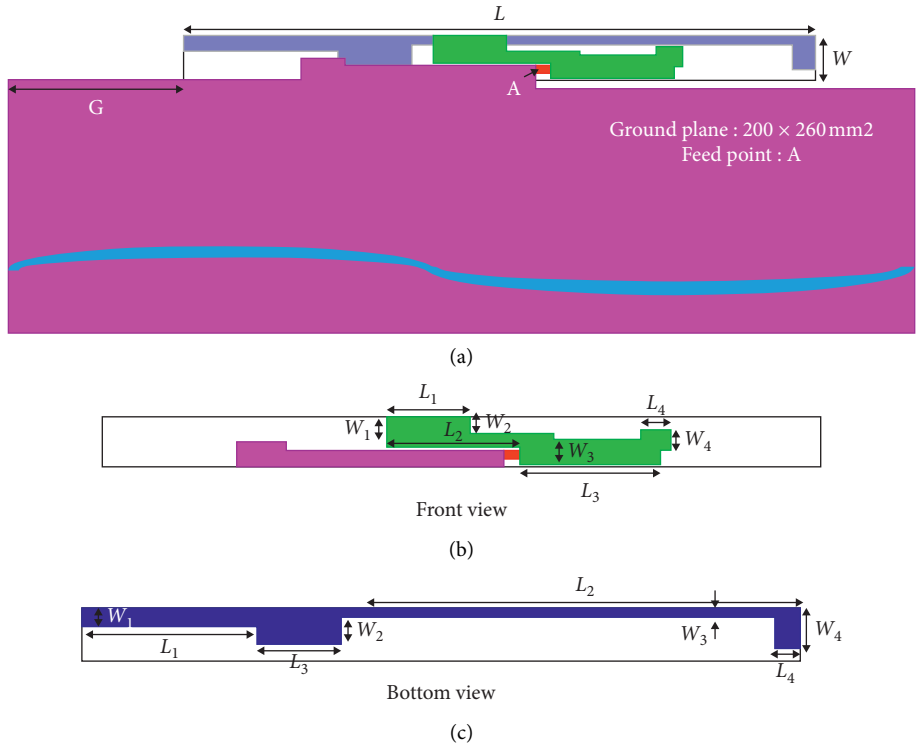

Figure 1: (a) Geometry of antenna; (b) front view of antenna geometry; (c) bottom view of antenna geometry.

Table 1: Dimensions of front of antenna.

Parameter	L	L_1	L_2	L_3	L_4	G	W	W_1	W_2	W_3	W_4
Value (mm)	43	5	8	8.4	1.8	12	3	1.8	1.0	1.45	1.2

Table 2: Dimensions of bottom of antenna.

Parameter	L_1	L_2	L_3	L_4	W_1	W_2	W_3	W_4
Value (mm)	10.5	26	5	1.5	1	1	0.5	2.25

(a) (b)

Figure 2: Continued.

(c)

Figure 2: Prototype antenna: (a) full front view; (b) partial front view; (c) bottom view.

laptop was simulated by a $200 \times 260\ mm^2$ copper plate. The antenna was designed to be placed on the top of the screen of a notebook computer. Figure 3 presents the components of the antenna. The couple-fed right arm excites the fundamental $\lambda/4$ resonant mode at 2.45 GHz, the higher $3\lambda/4$ resonant mode at 5.825 GHz, and the $5\lambda/4$ resonant mode at 6.85 GHz. The $3\lambda/4$ and $5\lambda/4$ resonant modes are controlled by the couple-fed left arm, and it can move to low frequencies. The $\lambda/4$ fundamental of 5.16 GHz is excited by the direct-fed left arm, and the couple-fed left arm controls the matching at 5.825 and 6.85 GHz. The integration of the three wide modes at 5.16, 5.825, and 6.85 GHz can create an operating range of 5.15–7.125 GHz (bandwidth of 1.975 GHz or 32.18%). This bandwidth covers the 5G WLAN and Wi-fi 6E application bands. The 2.45 GHz $\lambda/4$ fundamental mode is excited by the couple-fed right arm to cover 2.4 G WLANs (2.4–2.484 GHz). To test the performance of the antenna, a woven coaxial cable (characteristic impedance of 50 Ω) with a copper core is soldered onto the direct-fed right arm to supply the radio frequency signal.

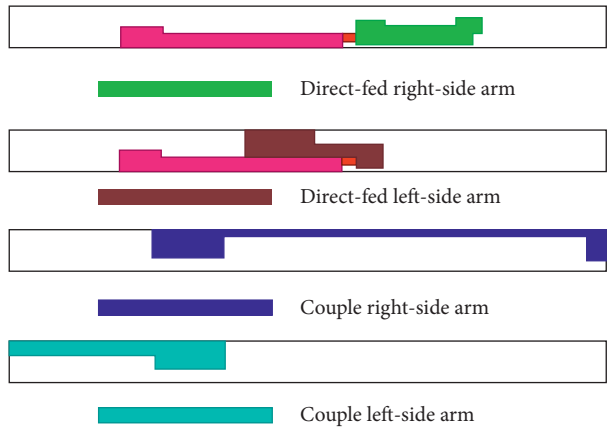

Figure 3: Components of antenna.

3. Experimental Results and Parametric Study

Simulations were conducted using Ansys HFSS software to obtain the S_{11} values used in this study. As shown in Figure 4, the measurements indicated good performance. The S_{11} value was −10 dB for covering the WLAN and Wi-fi 6E systems. Figure 5(a) presents the length of the couple-fed right arm and the various simulated S_{11} values. When the length of the couple-fed right arm was decreased by 1.5 and 3.0 mm, the 2.45 GHz fundamental mode shifted to a higher frequency, and the 2.4 GHz higher $3\lambda/4$ mode at 5.825 GHz and $5\lambda/4$ mode at 6.85 GHz also shifted to higher frequencies, resulting in a mismatch. Figures 5(b)–5(d) display the current distribution of the couple-fed right arm at 2.45, 5.825, and 5.85 GHz. For the resonant mode at 2.45 GHz, one null on the couple-fed right arm was observed, as shown in Figure 5(b). Therefore, the 2.45 GHz mode was in the $\lambda/4$ fundamental mode. For the resonant mode at 5.825 GHz, two nulls on the couple-fed right arm were observed, as shown in Figure 5(c). Therefore, the frequency is 5.825 GHz in the 2.45 GHz higher $3\lambda/4$ mode. For the resonant mode

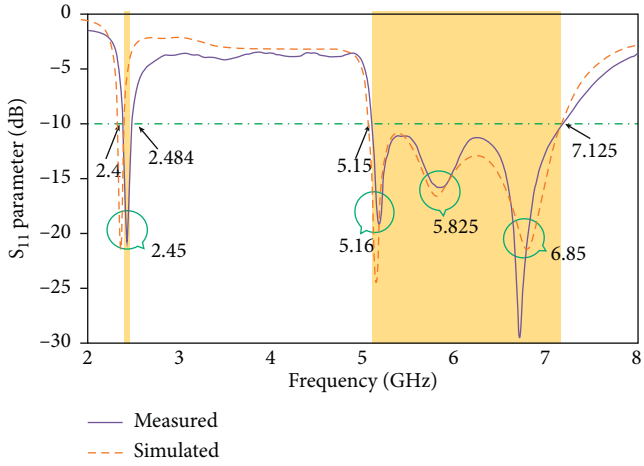

Figure 4: S_{11} values derived from simulation and measurement.

with 6.85 GHz, three nulls were observed on the couple-fed right arm, as shown in Figure 5(d). Therefore, the frequency is 6.18 GHz in the 2.45 GHz higher $5\lambda/4$ mode.

The simulated S_{11} values in Figure 6 indicate the different lengths of the couple-fed left arm. When the arm was

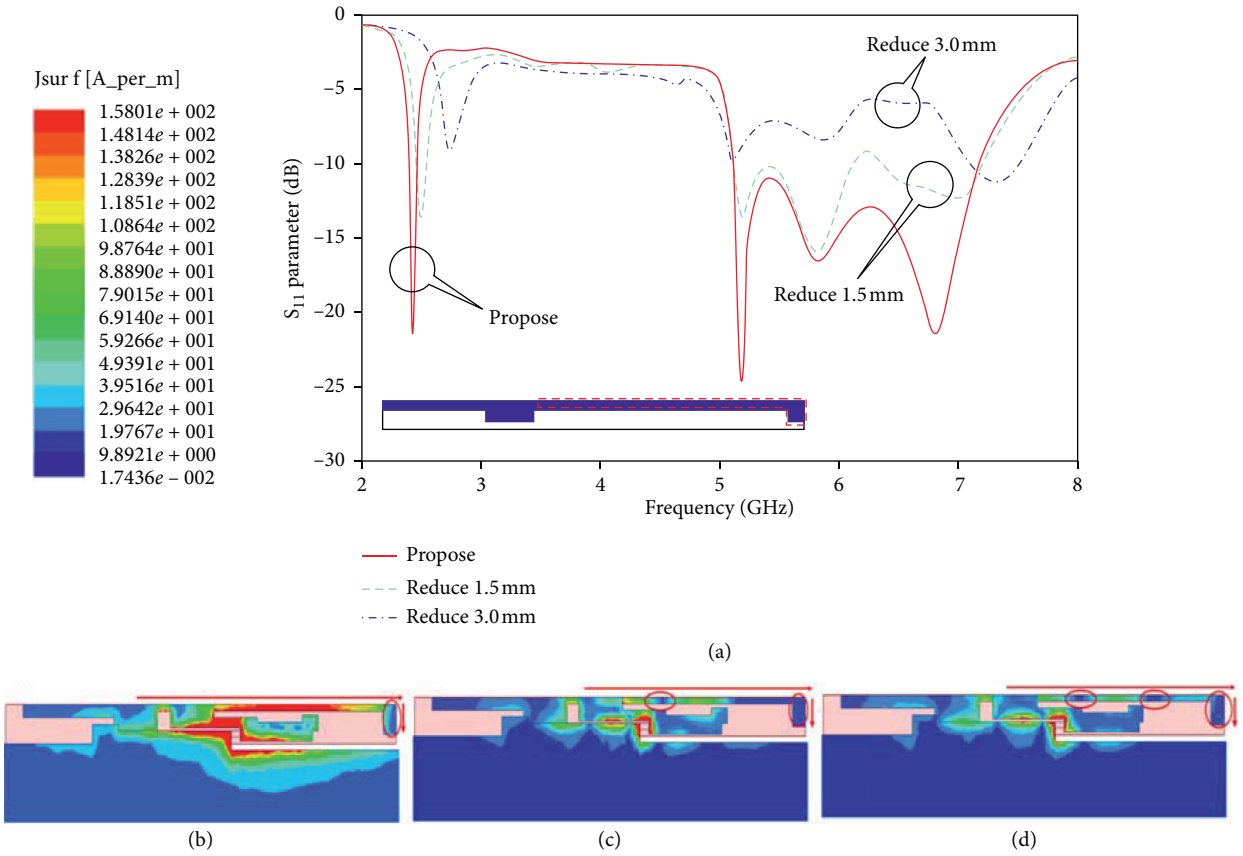

FIGURE 5: (a) Simulated S_{11} with different lengths of couple-fed right arm of the antenna. Current distribution of couple-fed right arm at (b) 2.45, (c) 5.825, and (d) 6.85 GHz.

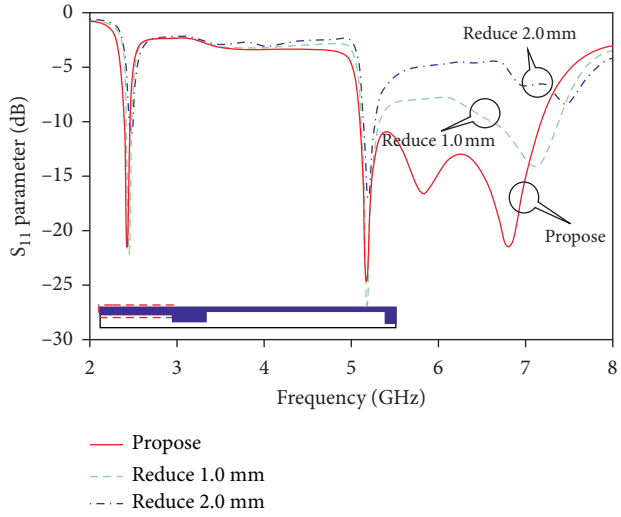

FIGURE 6: Simulated S_{11} with different lengths of couple-fed left arm of antenna.

shortened by 1 and 2 mm, 5.825 GHz and 6.85 GHz shifted to a higher mode and caused a mismatch. As mentioned previously, the couple-fed right arm's current distribution at 2.45 GHz resulted in frequencies of 5.825 and 6.85 GHz and a short couple-fed right arm phenomenon. This result confirms that the couple-fed right arm excites the fundamental at 2.45 GHz in the $\lambda/4$ resonant mode, 5.825 GHz in the $3\lambda/4$ resonant mode, and 6.85 GHz in the $5\lambda/4$ resonant mode.

The data in Figure 7(a) indicate the simulated S_{11} values resulting from reducing the length of the direct-fed left arm. The fundamental mode with this arm was excited at 5.16 GHz. The 5.16 GHz resonant mode shifted to higher frequencies when the length of the arm was reduced by 1.0

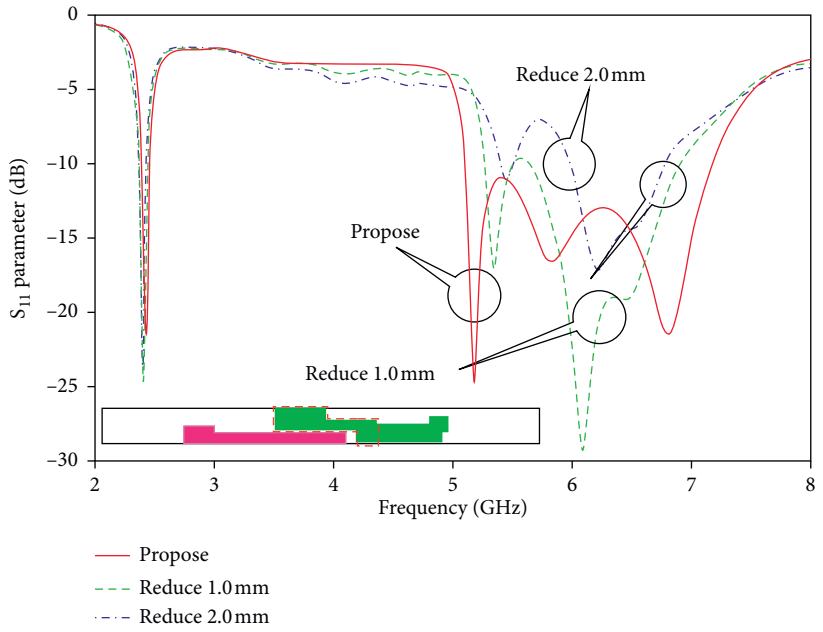

(a)

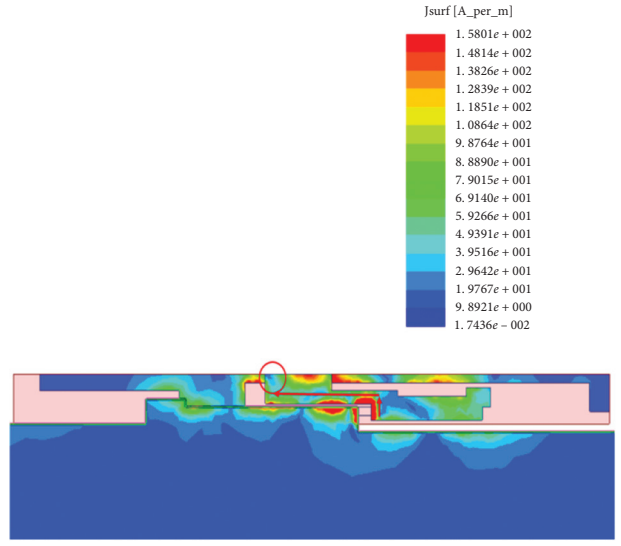

(b)

Figure 7: (a) Simulated S_{11} values with different lengths of direct-fed left arm of antenna. (b) 5.16 GHz current distribution of arm.

and 2.0 mm. Figure 7(b) presents a simulation of the direct-fed left arm and current distribution at 5.16 GHz. One null was observed in the arm. Thus, the 5.16 GHz fundamental mode was $\lambda/4$. Observed direct-fed left-side arm had one null. Thus, the 5.15 GHz fundamental mode was 1/4 λ.

The simulated S_{11} values presented in Figure 8 were derived from the different lengths of the direct-fed right arm. This can influence high band matching. When the length of the arm was reduced by 1 and 2 mm, mismatches occurred at 5.16, 5.825, and 6.85 GHz.

Figure 9 presents the simulated and measured of antenna radiation patterns in the *x-y*, *x-z*, and *y-z* planes at 2.45, 5.16, 5.825, and 6.85 GHz. In the *x-y* plane at 2.45 and 5.16 GHz, the radiation pattern was nearly omnidirectional. Therefore, 2.45 and 5.16 GHz are the fundamental $\lambda/4$ modes. Figure 10 presents the measured gain and efficiency of the antenna at 2400–2484 and 5150–7125 MHz. The antenna gain was 1.24–2.14 dBi (0.9-dBi variation), and the efficiency was 62.7%–68.9% (6.2% variation) at 2400–2484 MHz. The gain was above 1.13 dBi, and the efficiency was 53.4%–63.1% (9.7% variation) at 5150–5850 MHz. The gain was above 0.8 dBi, and the efficiency was 55.4%–68.6% (13.2% variation) at 5925–7125 MHz. Table 3 presents the measured gain, efficiency, resonant frequency, and bandwidth. As discussed, the antenna exhibited stable gain, high efficiency, and favorable radiation pattern.

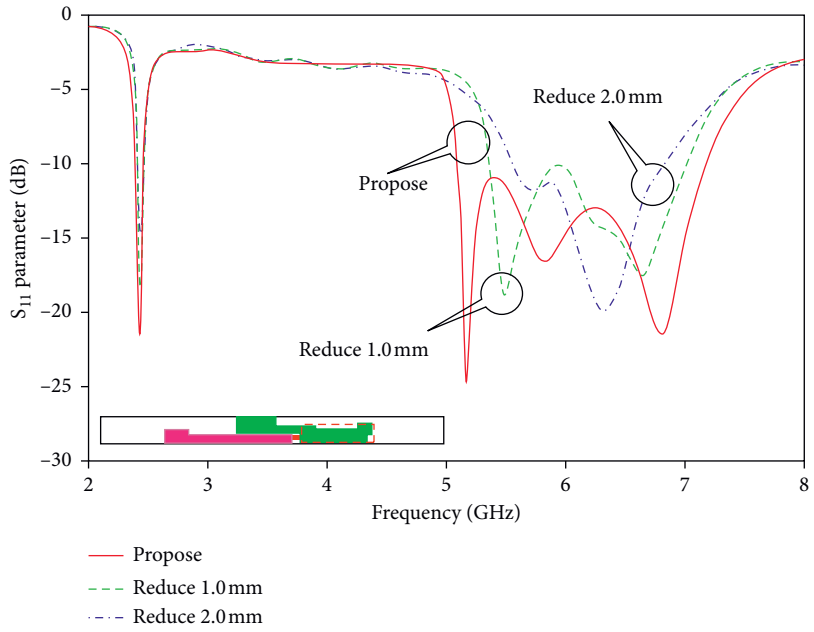

Figure 8: Simulated S_{11} values with different lengths of direct-fed right arm of antenna.

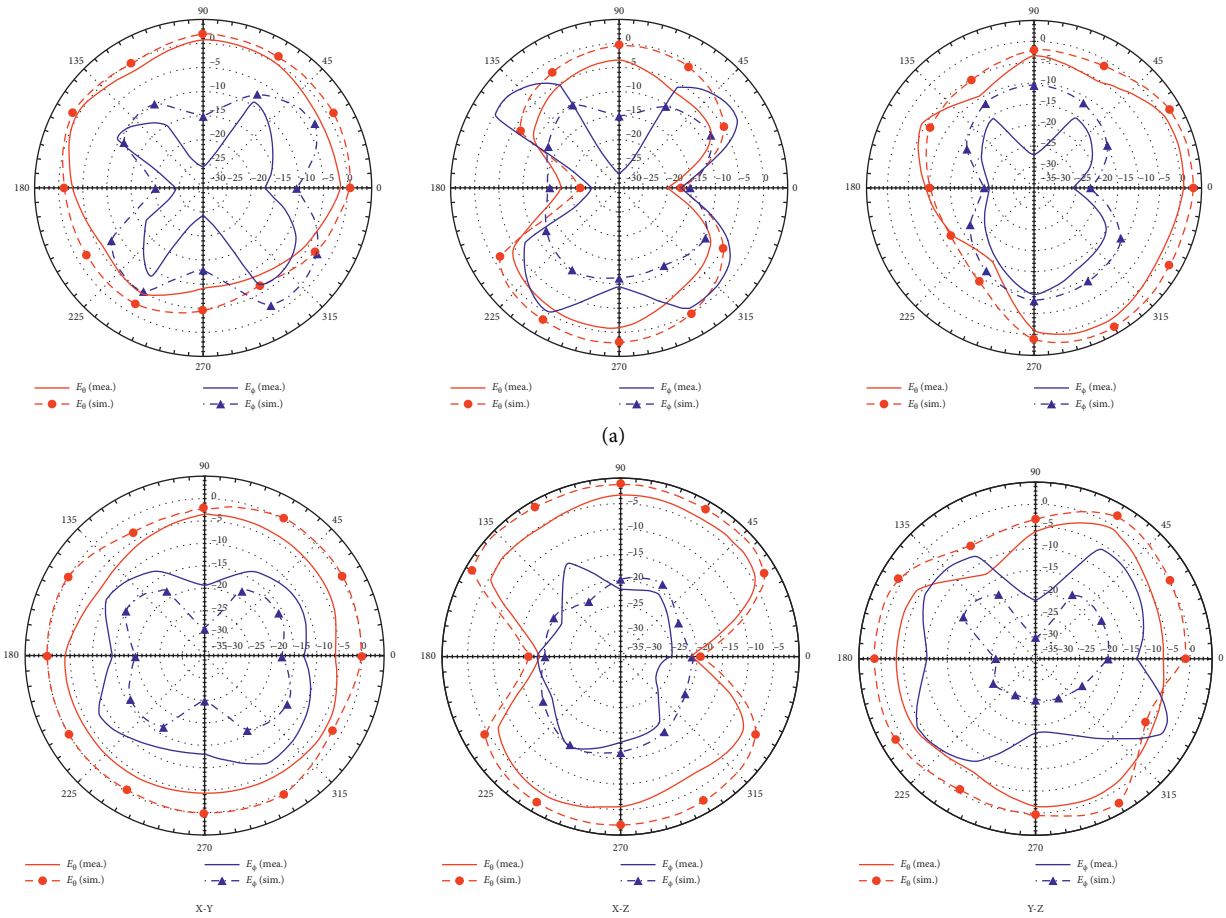

Figure 9: Continued.

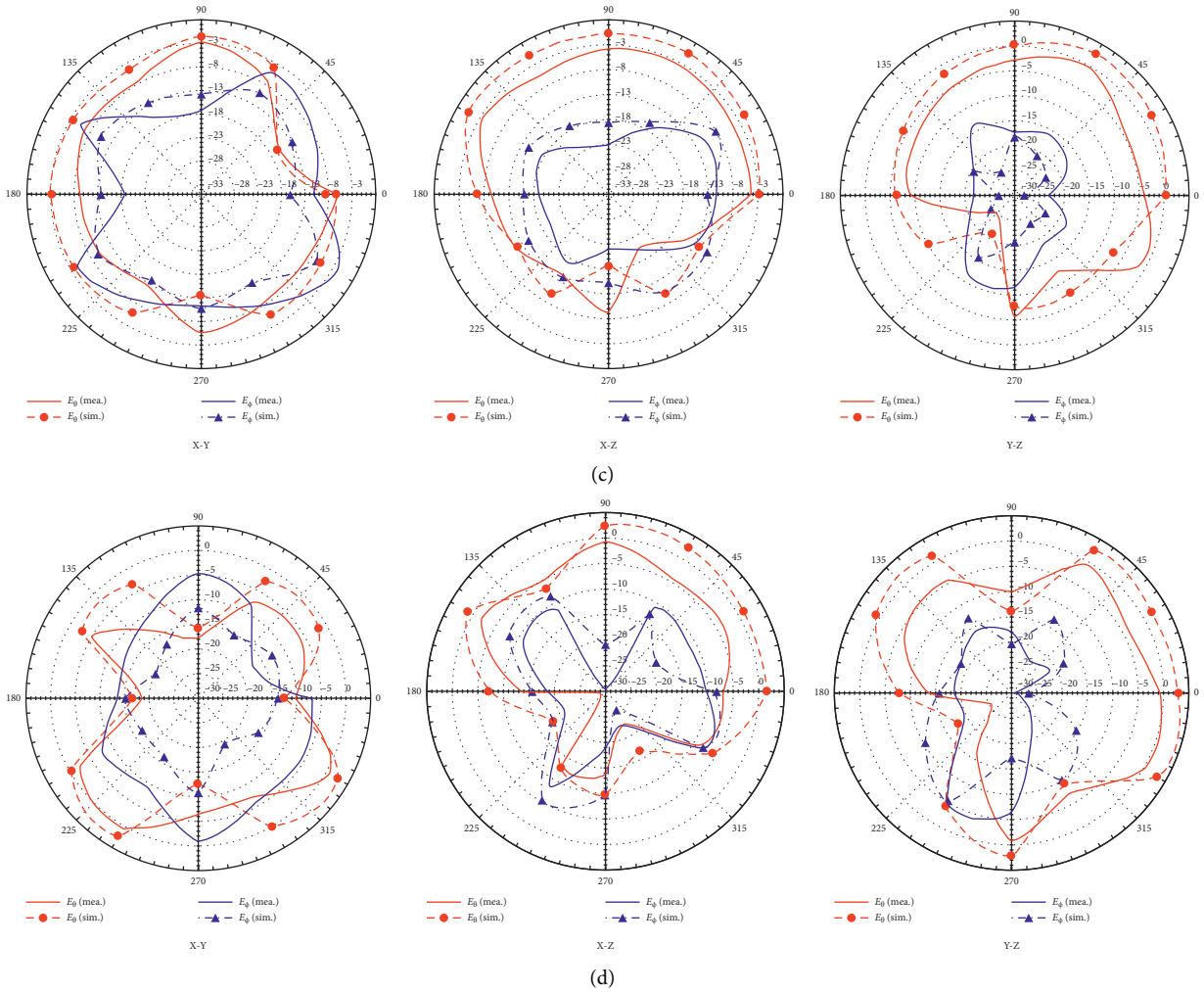

FIGURE 9: Two-dimensional radiation patterns of the antenna in the *x-y*, *x-z*, and *y-z* planes at (a) 2.450, (b) 5.16, (c) 5.825, and (d) 6.85 GHz.

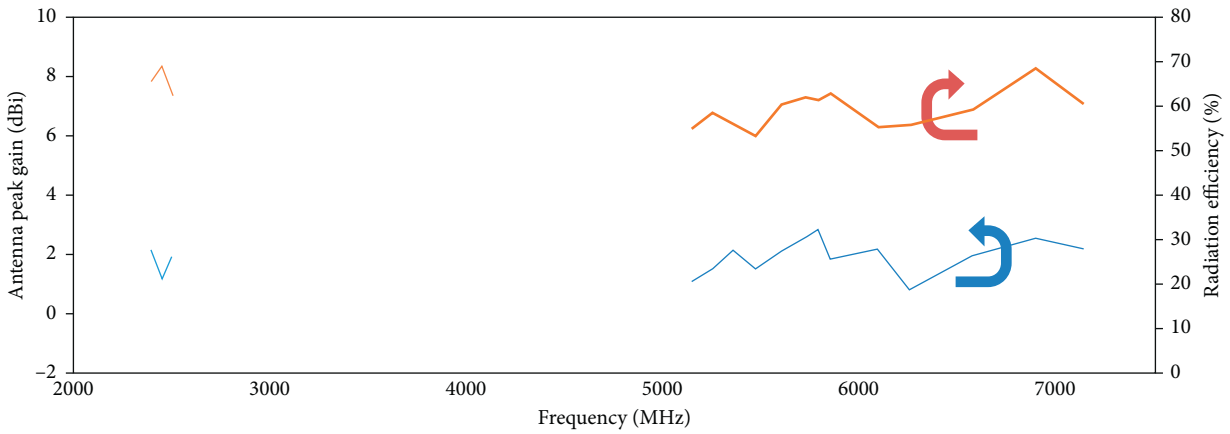

FIGURE 10: Measured of fain and radiation efficiency of antenna at 2400–2484 and 5150–7125 MHz.

To compare the performance of the antenna with that of other antennas, Table 4 presents the dimensions, w/wo chip element, support bandwidth, and dimension comparison. In [6–8], the PIFA structure was used to achieve small size antenna design. However, W parameter is larger than proposed antenna not suitable for current narrow-border products. In addition, antenna support bandwidth is less than proposed antenna. In [10–12], the authors used chip

Table 3: Resonant frequency, gain, efficiency, and bandwidth of antenna.

Resonance frequency (GHz)	Variation peak gain (dBi)	Variation efficiency (%)	Variation BW (GHz)
2.45	0.9 (1.24–2.14)	5.8 (62.7–68.9)	0.84 (2.4–2.484)
5.16 and 5.825	1.03 (1.13–2.15)	9.7 (53.4–63.1)	0.7 (5.15–5.85)
6.85	1.76 (0.82–2.84)	13.1 (55.42–68.6)	1.2 (5.925–7.125)

Table 4: Comparison of proposed antenna with other antennas.

References	Dimension $L \times W$ (mm)	Chip element	Bandwidth (MHz)	Dimension comparison (%)
[6]	21×8	N	2400–2484/3250–3420/5000–5920	130
[7]	5.4×9.7	N	2350–2510/4900–6000	40
[10]	30×4	Y	2400–2484/5150–5825	93
[11]	20×5	Y	2400–2484/5150–5825	77
[12]	12×5	Y	2400–2484/5150–5825	46
[8]	20.5×5	N	2400–2484/5150–5825/	79
[9]	46.5×9.3	N	2400–2484/5150–5825/	335
Present antenna	43×3	N	2400–2482/5150–5825/5825–7125	

element to achieve small size and narrow boarder antenna design. However, the use of inductor makes the hardware complex and also increases the difficulty of the manufacturing process. In [9], the antenna dimensions were larger than proposed antenna and support bandwidth was less than proposal antenna. Our proposed antenna dimension compared with reference is not the smallest, but the parameter of W, support bandwidth, and easily manufacturing process are suitable for current narrow-border products.

4. Conclusions

This study developed a small (43×3 mm^2) planar antenna for narrow-border notebook computers. The antenna covers the frequency ranges of 2.4–2.484 and 5.15–7.125 GHz by using two fundamental modes and two higher modes. The antenna support range includes those of the WLAN and Wi-fi 6E systems. The antenna is small, supports wide bands, has an omnidirectional radiation pattern at 2.45 and 5.16 GHz, and exhibits stable gain and high efficiency. According to the results, the antenna is suitable for narrow-border laptops.

Data Availability

The data used to support the findings of the study are available from corresponding author upon request.

Conflicts of Interest

The authors declare that they have no conflicts of interest.

References

[1] S. Jo, H. Choi, B. Shin, S. Oh, and J. Lee, "A CPW-fed rectangular ring monopole antenna for WLAN applications," *International Journal of Antennas and Propagation*, vol. 2014, Article ID 951968, 6 pages, 2014.

[2] C.-H. Chiu, C.-C. Lin, C.-Y. Huang, and T.-K. Lin, "Compact dual-band dipole antenna with asymmetric arms for WLAN applications," *International Journal of Antennas and Propagation*, vol. 2016, Article ID 195749, 4 pages, 2014.

[3] J. Bao, Q. Huang, W. Xinhuai, and X. Shi, "Compact multiband slot antenna for WLAN/WiMAX operations," *International Journal of Antennas and Propagation*, vol. 2014, Article ID 806875, 7 pages, 2014.

[4] A. S. Al-Zayed and V. A. Shameena, "Planar dual-band monopole antenna with an extended ground plane for WLAN applications," *International Journal of Antennas and Propagation*, vol. 2016, Article ID 6798960, 10 pages, 2016.

[5] W.-S. Chen, C.-M. Cheng, D.-H. Lee, and C.-L. Ciou, "Weisyun sin, and guang-yuan cai, "small-size meandered loop antenna for WLAN dongle devices," *International Journal of Antennas and Propagation*, vol. 2014, Article ID 897654, 7 pages, 2014.

[6] J. Kulkarni and V. Raju Seenivasan, "Design of a novel triple band monopole antenna for WLAN/WiMAX MIMO applications in the laptop computer," *International Journal of Antennas and Propagation*, vol. 2019, Article ID 7508705, 11 pages, 2019.

[7] C.-Y.-D. Sim, C.-C. Chen, X. Y. Zhang, Y.-L. Lee, and C.-Y. Chiang, "Very small-size uniplanar printed monopole antenna for dual-band WLAN laptop computer applications," *IEEE Transactions on Antennas and Propagation*, vol. 65, no. 6, pp. 2916–2922, 2017.

[8] S.-W. Su, C.-T. Lee, and S.-C. Chen, "Very-low-Profile, triband, two-antenna system for WLAN notebook computers," *IEEE Antennas and Wireless Propagation Letters*, vol. 17, no. 9, 2018.

[9] C.-C. Wan and S.-W. Su, "Compact, self-isolated 2.4/5-GHz WLAN antenna for notebook computer applications," *Progress in Electromagnetics Research M*, vol. 83, pp. 1–8, 2019.

[10] S.-W. Su, "Very-low-profile, 2.4/5-GHzWLAN monopole antenna for large screen-to-body-ratio notebook computers," *Microwave and Optical Technology Letters*, vol. 60, no. 5, pp. 1313–1318, 2018.

[11] S.-W. Su, C.-T. Lee, and S.-C. Chen, "Compact, printed, triband loop antenna with capacitively-driven feed and end-loaded inductor for notebook computer applications," *IEEE Access*, vol. 6, pp. 6692–6699, 2018.

[12] S.-W. Su, "Very-low-profile, small-sized, printed monopole antenna for WLAN notebook computer applications," *Progress In Electromagnetics Research Letters*, vol. 82, pp. 51–57, 2019.